International Journal of Refractory Metals & Hard Materials 72 (2018) 71–77

Contents lists available at ScienceDirect

International Journal of Refractory Metals & Hard Materials

journal homepage: www.elsevier.com/locate/IJRMHM

Effect of yttrium doping on the formation and stability of β-tungsten powder

Yazhou Hua, Jinshu Wang*, Jie Ma, Shuqun Chen, Chen Lai, Daniel den Englsen

Key Laboratory of Advanced Functional Materials, College of Materials Science and Engineering, Beijing University of Technology, Beijing 100124, China

ARTICLE INFO

Keywords:
β-W
Spray drying
Hydrogen reduction
DFT simulation

ABSTRACT

Yttrium oxide doped tungsten powders were produced by spray-drying solutions of ammonium metatungstate (AMT) and yttrium nitrate, calcining the spray dried powder, and reducing with hydrogen. During the reduction process, the formation of metastable β-tungsten (β-W) was observed; this phase was still present after being reduced at 950 °C whereas β-W was not found upon reducing pure tungsten oxide at the same conditions. The effect of Y-doping on the synthesis and stability of β-W was investigated by using density functional theory simulation. Our calculation results indicate that the formation energy of Y doped β-W is lower than that of undoped β-W. Charge density analysis further revealed the formation of a covalent structure of Y-O-W between substitutional Y, interstitial O and adjacent W in β-W, which traps the oxygen atom at an interstitial site in the β-W instead of being desorbed. This structure improves the stability of β-W substantially.

1. Introduction

Tungsten has a high melting point, high hardness, strong wear resistance, low coefficient of thermal expansion, excellent thermal conductivity and good corrosion resistance, which explains its wide application in many fields [1–4]. Tungsten has two different cubic structures, α-W (cubic, space group: Im-3m) and β-W (cubic, space group: Pm-3n), of which the lattice constants are 3.165 Å and 5.05 Å, respectively [5,6]. These two phases exhibit many different functional properties; for example, the electrical conductivity of α-W is superior to β-W, while the superconducting transition temperature for α-W at 15 mk is much lower than the transition temperature (between 1and 4 k) for β-W [7–9]. In contrast to α-W, which is very stable due to the bcc(A2) structure, β-W has the less stable A15 structure and will transform to α-W at low-temperature annealing; the transition temperature is between 520–625 °C [10,11].

The formation and stability of β-W are determined by many factors, such as reduction temperature, humidity and flow rate of hydrogen, the thickness of the material layer, the kind and concentration of impurity elements. Morcom et al. [11] studied the effect of the WO_3 specific surface area on the formation of β-W in 1974. The results showed that it was only possible to obtain pure β-W when the specific surface area of WO_3 was large otherwise a mixture of β-W and $WO_{2.9}$ was obtained. Huang et al. [12] studied the hydrogen reduction process of pure WO_3 powder at 500 °C; they found that the formation of β-W was extremely sensitive to the hydrogen flow rate. In spite of these observations, some other studies claimed that the β-W phase did not appear during hydrogen reduction of tungsten oxide [13–15].

Recently, the large Hall effect discovered in β-W films has sparked renewed interest in this phase, because it can be potentially utilized to switch the ferromagnetic layers in a tunnel magnetoresistance TMR device [16–18]. By exploiting the superconducting properties of β-W, novel spintronic devices could be developed in the future. Many techniques have been utilized to synthesize thin films of β-W such as sputtering, electron-beam evaporation, electrolysis, chemical vapor deposition (CVD) and reduction of WO_3 by hydrogen [19–22]. The latter process is the most productive way to produce high-quality β-W; however, at temperatures between 520–625 °C β-W normally transforms to α-W automatically. In our study we synthesized stable β-W for the first time by hydrogen reduction of yttrium oxide doped tungsten oxide. The introduction of the rare earth element Y has been found to extend the temperature range for the stability of β-W considerably. It is the objective of the present study to determine the mechanism of this improved stability.

2. Experimental

Commercial ammonium meta-tungstate (AMT), $[(NH_4)_6(H_2W_{12}O_{40})_4H_2O]$ (99.9% pure) and yttrium nitrate were separately dissolved into deionized water before mixing together. The samples containing 0.5 wt%, 1 wt%, 2.5 wt%, 5 wt%, and 10 wt% yttrium, were denoted as Y0.5, Y1, Y2.5, Y5, and Y10, respectively. The Eyela SD-1000 spray dryer was employed to prepare precursor mixed powder by spray-drying the mixed solution containing AMT and $Y(NO_3)_3$. The

---

* Corresponding author.
E-mail address: wangjsh@bjut.edu.cn (J. Wang).

https://doi.org/10.1016/j.ijrmhm.2017.12.006
Received 6 June 2017; Received in revised form 16 November 2017; Accepted 6 December 2017

precursor powder was calcined at 650 °C for 150 min in air to remove organic components. The obtained powder was ground and sieved with a 150-mesh standard sieve. Hydrogen gas was used to reduce the doped tungsten oxide into tungsten at various temperatures, to be described in the next section. These experiments were carried out in a tube furnace, in which the powders were placed in a molybdenum boat. The hydrogen flow rate was 360 ml/s, and the heating rate was set at 10 °C/min. The annealing temperature was kept for 45 min, then the furnace was cooled down. The thermal analysis experiments of the precursor powder were carried out using a simultaneous thermal analyzer (NETZSCH STA 449C) under nitrogen atmosphere at heating rates of 10 °C min^{-1} from room temperature to 1000 °C. The phase analysis of the reduced powders was carried out using X-ray diffraction (XRD, Bruker D8) with Cu k_α (λ = 0.154056 nm) radiation. The morphology of the powders was examined by field-emission scanning electron microscope (FE-SEM, Hitachi S4800) and high-resolution transmission electron microscopy (HRTEM, Hitachi H-700). The chemical state of elements was investigated by the X-ray photoelectron spectrum (XPS, PHI Quantera SXM).

3. Results and discussion

3.1. Decomposition process of precursor powder

The precursor powder prepared by spray drying normally contains a large amount of nitrate and ammonia compounds. In the reduction process, NO_2 produced by nitrate decomposition will react with tungsten oxide, which is detrimental to the reduction of tungsten oxide. So it is necessary to calcine the precursor powder at high temperature to remove unnecessary ions. In order to determine the optimum calcination temperature, we studied the decomposition process of the precursor powders of the sample Y10 by thermogravimetric (TG) and differential scanning calorimetry (DSC) analyses. The TG- and DSC-curves of Y10 and AMT are shown in Fig. 1. The TG curve of Y10 can be divided into three stages, stage A, stage B, and stage C, corresponding to the temperature regions of 60 °C–230 °C, 230 °C–320 °C and 320 °C–585 °C respectively, as shown in Fig. 1(a). On the other hand, the TG curve of AMT can be divided into three stages, stage D, stage E, and stage F, corresponding to the temperature regions of 50 °C–200 °C, 200 °C–370 °C and 370 °C–500 °C, respectively, as shown in Fig. 1(b). In the stage A, a dehydration process occurred, which caused 5% weight loss, showing also clearly its endothermic character with the broad peak about 127 °C in the DSC curve. This is mainly due to the loss of intergranular water adsorbed by powders and partially crystal water of yttrium nitrate. In Fig. 1(b), the TG- and DSC-curves of stage D support the above statement. Two peaks at 267 °C and 300 °C in the DSC-curve along with 10% weight loss indicated by the TG-curve were detected in stage B. The exothermic peak at 267 °C is due to the formation of intermediate $YONO_3$ by decomposing $Y(NO_3)_3$ [23]. The endothermic peak around 300 °C of stage B and stage E can be attributed to the decomposition of AMT, which leads to the evaporation of ammonia and crystal water [24]. When the temperature was increased to 532 °C, the DSC-curve indicates the endothermic decomposition of $YONO_3$ to Y_2O_3. Finally, an exothermic peak at 585 °C can be observed, which might be attributed to breaking down the metal clusters in AMT [25]. This result is higher than the reported temperatures in earlier literature (417–439 °C) [25] and the observed temperature in Fig. 1(b), in which the exothermic peak was found at 425 °C accompanied with a 1.7% weight loss. The temperature for breaking the metal cluster increases, which may be due to the introduction of yttrium nitrate that stabilizes the metal clusters. The endothermic reaction during the decomposition process of yttrium nitrate hinders the transition of AMT structure. At the end of stage C no peaks were observed in either the TG- or DSC-curves, indicating that the nitrate and ammonia compounds were completely decomposed. Based on these observations, the calcination temperature was set at 650 °C to remove any residual nitrate and ammonium ions. Based on the discussion above, the reactions involved during thermal decomposition can be described by the chemical Eqs. (1) and (2) given below.

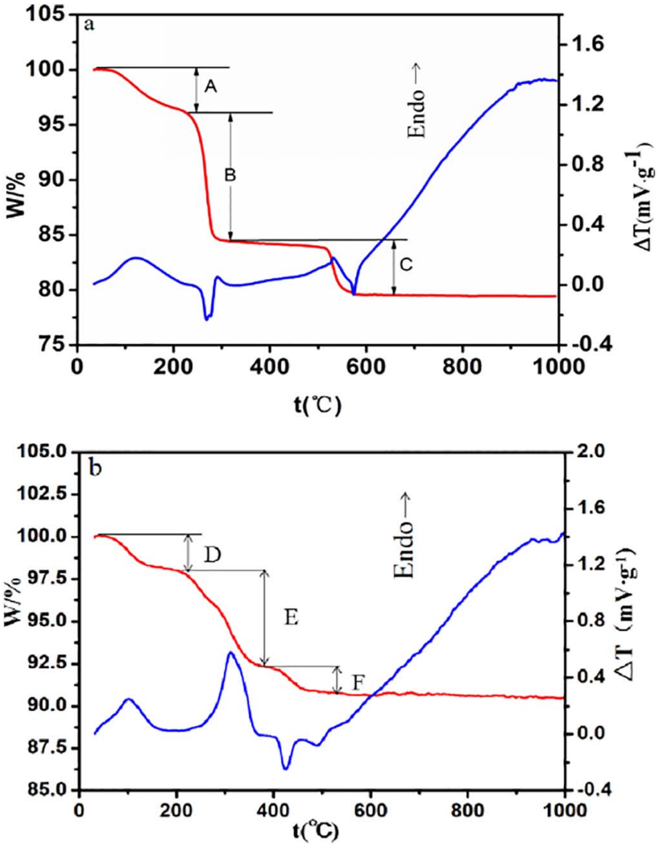

Fig. 1. TG- and DSC-curves of the spray-dried powders: (a)Y10; (b)AMT.

$$(NH_4)_6H_2W_{12}O_{40}\cdot 4H_2O \rightarrow 6NH_3\uparrow + 12WO_3 + 8H_2O\uparrow \tag{1}$$

$$2[Y(NO_3)_3\cdot 4H_2O] \rightarrow Y_2O_3 + 6NO_2\uparrow + 8H_2O\uparrow + 3O_2\uparrow \tag{2}$$

Fig. 2 shows XRD pattern of oxide powders calcinated at 650 °C for 150 min. The oxide powders are mainly composed of WO_3 phase and $WO_{2.9}$ phase. This indicates AMT is completely decomposed at this temperature. Meanwhile, Y_2WO_6 phase is also observed in the pattern, which may result from the reaction of WO_3 and Y_2O_3.

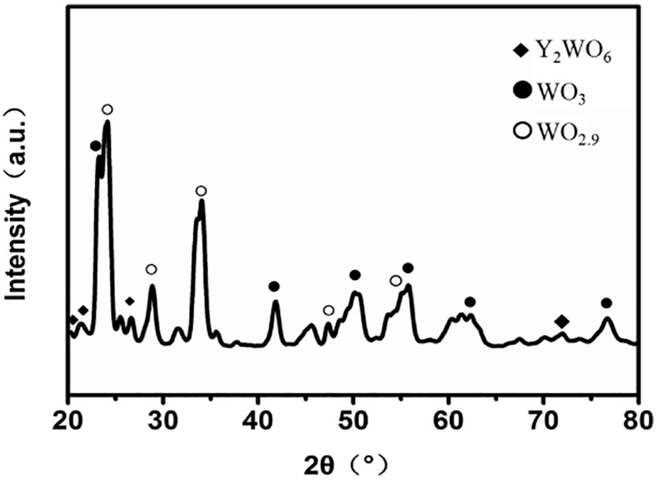

Fig. 2. XRD pattern of the Y10 sample after calcination at 650 °C.